Perpendicular Spin Orientation in Ultrasmall Fe Islands on W(110)

R. Röhlsberger,[1] J. Bansmann,[1] V. Senz,[1] K. L. Jonas,[1] A. Bettac,[1] O. Leupold,[2]
R. Rüffer,[2] E. Burkel,[1] and K. H. Meiwes-Broer[1]

[1]*Universität Rostock, Fachbereich Physik, Universitätsplatz 3, 18055 Rostock, Germany*
[2]*European Synchrotron Radiation Facility, B.P. 220, 38043 Grenoble Cedex, France*

(Received 7 November 2000)

We have studied the magnetism of Ag-coated Fe islands on W(110) by nuclear resonant scattering of synchrotron radiation at the 14.4 keV resonance of ^{57}Fe. Separated islands with an average diameter of 2.0 nm and monolayer thickness are formed at a Fe coverage of $\theta = 0.57$ bulk monolayers. Time spectra of the nuclear decay were measured in the temperature range from 4.5 to 300 K. We find strong evidence for perpendicular spin orientation, which most likely results from the interplay of shape anisotropy and elastic strain in the islands.

DOI: 10.1103/PhysRevLett.86.5597 PACS numbers: 75.70.Ak, 76.80.+y

The magnetism of self-organized nanostructures and clusters is an active field of research due to a rich variety of novel properties that are not found in the bulk [1,2]. An understanding of these properties is highly desirable because of fundamental aspects of nanoscale magnetic ordering in general and possible applications in high-density magnetic storage and magnetoelectronics in particular. Magnetic order in low-dimensional systems like thin films is induced by anisotropies resulting from broken local symmetries. A striking phenomenon in low-dimensional magnetism is the perpendicular spin orientation in *ultrathin* films. Despite extensive experimental and theoretical efforts, a complete understanding of the relevant anisotropies has not been achieved so far. Qualitatively, the magnetization direction is determined by the interplay of surface and shape anisotropies and usually forces the magnetic moment into the film plane. If, however, the balance between these quantities is changed, a change of the magnetization direction can occur from an in-plane orientation to an orientation out of plane. A number of investigations in this field have been reported so far [3,4].

One of the first systems in which two-dimensional ferromagnetic ordering has been observed was the Fe monolayer on W(110) [4,5] that has been used as a model system for two-dimensional magnetism since then. Magnetic ordering in this system has been studied by Mössbauer spectroscopy [5,6], spin-polarized low-energy electron diffraction [7,8], magnetometry [9], and spin-resolved photoelectron spectroscopy [10]. Because of the high surface energy of the W substrate in comparison with that of the film, the Fe monolayer on W(110) is thermodynamically stable, in contrast to other layer/substrate systems like Fe/Cu and Fe/Ag. As a result of the large misfit between the Fe and W lattices of -9.4%, the pseudomorphic Fe monolayer on W(110) is completed at a coverage of $\theta = 0.82$ [measured in units of one bulk Fe(110) monolayer]. The magnetization of this monolayer is confined to the film plane with a pronounced twofold anisotropy, the easy axis pointing along the $[1\bar{1}0]$ directions [11]. Coverages below $\theta = 0.58$ lead to formation of stable and well separated pseudomorphic islands [12]. There are only a few studies of this system reported so far. To some extent the relation between magnetism and morphology of these islands was investigated by Elmers *et al.* down to temperatures of 115 K [13]. The separated islands appeared to be nonmagnetic due to superparamagnetic relaxation. However, the magnetic order of these islands at low temperatures has not been studied so far.

In this Letter we report on magnetic ordering in ultrasmall pseudomorphic Fe islands on W(110) at temperatures as low as 4.5 K and present strong evidence for a perpendicular spin orientation. We have probed the magnetism of the islands by *nuclear resonant scattering of synchrotron radiation* at the 14.4 keV resonance of ^{57}Fe. Compared to classical Mössbauer spectroscopy, this technique exhibits qualitatively new features. In particular, the pulsed time structure suggests to perform hyperfine spectroscopy on a time scale rather than on an energy scale: The simultaneous excitation of the hyperfine-split nuclear energy levels by a radiation pulse leads to quantum beats in the temporal evolution of the subsequent nuclear decay signal. The analysis of this beat pattern allows a precise determination of the magnitude and the orientation of magnetic fields in the sample [14]. As a microscopic probe, this technique provides complementary information to methods like magneto-optical spectroscopy or x-ray dichroism. Because of the extremely high brilliance of the undulator synchrotron radiation at third-generation facilities it offers unique possibilities to probe magnetic properties with monolayer sensitivity [15].

Our samples were prepared under ultrahigh-vacuum conditions by thermal evaporation of Fe, enriched to 95% in ^{57}Fe, on an atomically clean W(110) crystal at 450 K. The cleanliness of the W(110) surface and the pseudomorphic growth of the Fe islands were controlled by low-energy electron diffraction (LEED). The morphology of the islands was then inspected by scanning tunneling microscopy (STM). An STM image of the sample studied here is shown in Fig. 1. The coverage was determined from several STM images to be $\theta = 0.57$ which is slightly

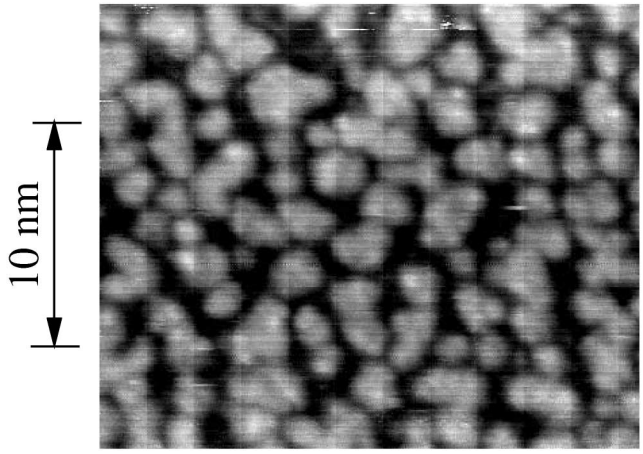

FIG. 1. STM image of Fe islands prepared on W(110) at 300 K before deposition of the Ag cap. The Fe coverage corresponds to $\theta = 0.57$ bulk monolayers.

below the percolation limit. In an approximation of the islands by circular disks, their average diameter was determined to be $r_{\text{ave}} = 2.0$ nm. After preparation the sample was coated with about five monolayers of Ag to prevent contamination in the subsequent *ex situ* experiment.

The experiments were carried out at the nuclear-resonance beam line ID18 of the European Synchrotron Radiation Facility [16]. To facilitate time-resolved measurements, the storage ring was operated in 16-bunch mode, providing a time interval of 176 ns between subsequent bunches. An energy bandwidth reduction to 6.5 meV by a high-resolution monochromator prevented the detector from being overloaded by the huge intensity of nonresonant photons. The sample was mounted in a He cryostat with the in-plane [001] direction aligned parallel to the incident beam. It was illuminated in a vertical scattering geometry at an angle of 5 mrad, the critical angle of total reflection of the W substrate at 14.4 keV. In this geometry we obtained a total count rate of about 0.5 s^{-1} in the time window from 15 to 100 ns, including a background count rate (off resonance) of 0.05 s^{-1}, at an average electron beam current of 70 mA in the storage ring. The typical data acquisition time to acquire sufficient statistical quality in a time spectrum was about 2 h. A series of time spectra taken at various temperatures is shown in Fig. 2. The decay of the time-resolved reflectivity is considerably faster than the natural decay that is shown as the dotted line in the top picture. With decreasing temperature an additional modulation appears in the time spectra that results in distinct peaks at $t_1 = 34$ ns and $t_2 = 68$ ns at 4.5 K.

For a theoretical description we approximate the frequency-dependent reflectivity of a very thin film of thickness d on a semi-infinite substrate by [17]

$$\mathbf{R}(\omega) \approx \exp[id|t_{02}(\varphi)|^2\mathbf{f}(\omega)/\varphi], \qquad (1)$$

where $t_{02}(\varphi)$ is the Fresnel transmission coefficient of the vacuum-substrate boundary at the angle of incidence φ.

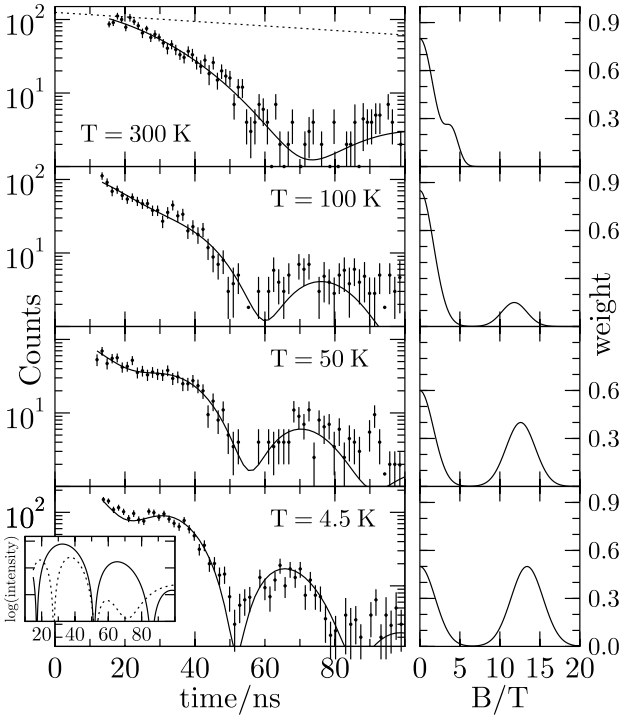

FIG. 2. Time spectra of nuclear resonant grazing-incidence reflection from ultrasmall ^{57}Fe islands on W(110). The modulation of the intensity is attributed to a perpendicular magnetization of the Fe islands. The solid lines are the results of simulations according to Eq. (1). The dotted line in the top graph represents the natural decay of the ^{57}Fe level. The inset shows calculated time spectra of the magnetic component in the case of perpendicular magnetization (solid line) and in-plane magnetization (dotted line) for a field of $B = 13.5$ T. The right panel displays the probability density for the hyperfine field distribution that was obtained from the simulations.

The reflectivity $\mathbf{R}(\omega)$ and the scattering amplitude $\mathbf{f}(\omega)$, denoted by boldface letters, are 2×2 matrices to account for the strong polarization dependence of the resonant scattering process. Equation (1) is similar to the description of nuclear forward scattering [18] from a sample with an "effective" thickness given by $d' = d|t_{02}(\varphi)|^2/\varphi$. This means that the intensity of the resonantly scattered radiation peaks at the critical angle of the substrate. The 14.4 keV transition of ^{57}Fe is a magnetic dipole transition with spins $I_g = 1/2, I_e = 3/2$, magnetic moments $\mu_g = 0.091\mu_N, \mu_e = -0.153\mu_N$ of the ground and excited state, respectively, and a natural lifetime of $\tau_0 = 141$ ns. A magnetic hyperfine interaction lifts the degeneracy of the magnetic sublevels which leads to six dipole-allowed transitions with different resonant energies. The matrix elements of the scattering amplitude in this case are given by [19]

$$[\mathbf{f}]_{ab} = \frac{3}{16\pi}\{(\hat{e}_a \cdot \hat{e}_b)[F_{+1} + F_{-1}] + i(\hat{e}_a \times \hat{e}_b) \cdot \hat{m}[F_{+1} - F_{-1}] + (\hat{e}_a \cdot \hat{m})(\hat{e}_b \cdot \hat{m})[2F_0 - F_{+1} - F_{-1}]\}, \qquad (2)$$

where the $F_\nu = F_\nu(\omega)$ are the energy-dependent resonant strengths for dipole transitions with a change in the magnetic quantum number of $\Delta m = \nu$. Each of the $F_\nu(\omega)$ describes two resonance lines with an energetic separation of $\hbar\Delta\omega = (\mu_g/I_g - \mu_e/I_e)B$, where B is the magnitude of the magnetic hyperfine field at the nucleus. $\hat{e}_a$ and $\hat{e}_b$ are unit vectors that are derived from the chosen polarization basis $(\hat{\boldsymbol{\epsilon}}_a, \hat{\boldsymbol{\epsilon}}_b)$ via $\hat{e} = \hat{\boldsymbol{\epsilon}} \times \hat{k}_0$. $\hat{k}_0$ is the unit wave vector of the incident photon and $\hat{m}$ describes the orientation of the magnetic hyperfine field. This formalism is part of the program package CONUSS that has been developed for the description of time-resolved nuclear resonant scattering of x rays [14], extended to grazing-incidence reflection from thin films [20]. In the simulations we have assumed a layer system consisting of a 0.2 nm thick film of ^{57}Fe on W. We chose a linear polarization basis with the σ polarization parallel to the plane of the storage ring. The right panel in Fig. 2 shows the distribution of magnetic fields that was obtained from the simulations. The strongly accelerated decay at 300 K is a result of the coherent nature of the scattering process. It is attributed to a broad distribution of hyperfine interactions around $B = 0$ T and a weak component around $B = 4$ T, as was already observed in the single monolayer Fe on W(110) [5,6]. The former component is found at all temperatures and is most likely related to parts of the sample that do not order magnetically in the temperature range investigated here. With decreasing temperature a nonzero magnetic component appears due to magnetic ordering of the Fe islands. The modulation in the time spectra is characteristic for a perpendicular magnetization. In this case the scattering matrix $\mathbf{f}$ is diagonal and the scattering response for incident σ polarization is given by $[\mathbf{f}]_{\sigma\sigma} = (3/8\pi)F_0$. Thus, we expect a single quantum-beat frequency in the time response, as discussed above. Taking the time difference of $t_2 - t_1 = 34$ ns of the maxima at 4.5 K as quantum-beat period Δt, we obtain for the magnetic field $B = h/[\Delta t(\mu_g/I_g - \mu_e/I_e)] = 13.5$ T. This value is slightly larger than the value of $B = 11.9(2)$ T that was extrapolated for the Ag-coated Fe monolayer on W(110) at 0 K [5]. Since the Curie temperature is very likely dependent on the island size, the size distribution leads to a distribution of magnetic hyperfine fields that accounts for the width of the magnetic component at a given temperature.

The right panel in Fig. 2 shows that the weight of the magnetic component increases with decreasing temperature. This is attributed to superparamagnetic relaxation of the magnetic moments [21]. At high temperatures the magnetization of small particles is subject to fast thermal fluctuations so that the effective magnetic hyperfine field averages to zero. The transition from the fast-relaxation regime to the magnetically ordered state occurs at a temperature that is roughly given by the condition $KV = k_B T$, where K is the magnetic anisotropy constant and V is the particle volume. However, due to the size distribution of the islands the transition extends over a rather broad temperature range. The temperature dependence of the weight of the magnetic component points to an average blocking temperature around 50 K. Taking an average island volume of $V = 0.6$ nm^3, we estimate an anisotropy constant of $K \approx 1.0 \times 10^6$ J/m^3. This is about 20 times the anisotropy constant of bulk Fe. Such an enhancement is attributed to the reduced symmetry of the system [22] and has been observed for other ultrathin films and nanoparticles as well [23].

An in-plane magnetization of the Fe islands can be excluded, because it cannot reproduce the relative intensities of the quantum-beat peaks observed here. For example, the intensity around $t = 65$ ns would be strongly suppressed, as shown in the inset in Fig. 2 (dotted line). In that geometry the four resonance lines belonging to the $\Delta m = \pm 1$ transitions contribute to the scattered amplitude, leading to $[\mathbf{f}]_{\sigma\sigma} = (3/16\pi)(F_{+1} + F_{-1})$. It should be noted here that a magnetization along exclusively one of the in-plane [001] directions could explain the measured data, too. However, this can be ruled out because the [001] and $[00\bar{1}]$ directions should be equally populated due to the superparamagnetic relaxation. Even after cooling below the superparamagnetic blocking temperature in a zero external field such a configuration would be energetically more favorable since it minimizes the magnetic stray field by flux closure of adjacent islands. Then the scattered amplitude is again given by the above expression with four resonance lines contributing. As a result of the above considerations, our data strongly indicate a perpendicular spin orientation of the islands. The solid lines in the left panel of Fig. 2 are the results of the simulation, assuming an incoherent superposition of the amplitudes scattered from the magnetic and the nonmagnetic component. This is reasonable if the lateral separation of these components on the sample is larger than the transverse coherence length of the radiation, which is estimated to be in the range of 30 nm in the scattering geometry used here [24].

The perpendicular magnetization of the Fe islands is quite remarkable because Fe films on W(110) are known to be magnetized in plane for coverages $\theta > 0.6$ [4]. In general, the perpendicular anisotropy of an ultrathin film can be written as $f_\perp = f_{\mathrm{Sh}} + f_{\mathrm{MC}} + f_{\mathrm{ME}}$, where f_{Sh} is the shape anisotropy, f_{MC} is the magnetocrystalline anisotropy, and f_{ME} is the magnetoelastic anisotropy that is proportional to the in-plane strain of the film [25]. If $f_\perp < 0$, a perpendicular magnetization of the film is preferred. In case of separated islands the balance between these contributions will be changed compared to a continuous film: First, due to the small island size the shape anisotropy f_{Sh} is significantly reduced, and, second, f_{ME} assumes a large negative value, most likely due to strain energies in the film. In case of Fe sesquilayers ($\theta = 1.5$) on W(110), f_{ME} was found to be about an order of magnitude larger than predicted from bulk elasticity theory [26]. This was identified as the origin for perpendicular spin orientations in the double-layer patches of this system [26]. At coverages $\theta < 0.58$ the separated Fe islands on W(110) may be in a similarly strained state, thus

favoring a perpendicular spin orientation as well. This is supported by the striking elastic behavior that has been observed recently by Sander *et al.* [27]. They found a sharp maximum of very strong *compressive* stress at coverages around $\theta = 0.6$, which is very close to the value of our sample. This suggests the islands to be in a state with a strong modification of the magnetoelastic coupling. Compared to the pseudomorphic monolayer, the elastic strain may be partially relaxed due to misfit dislocations, similar to the second layer of Fe atoms in the sesquilayers on W(110). At higher coverages and increasing coalescence between islands, *tensile* stress and the full pseudomorphic strain develop for which an in-plane magnetization is more favorable. However, a quantitative understanding of these magnetoelastic effects in the submonolayer range is still lacking. In a detailed analysis also the influence of the nonmagnetic coating has to be taken into account that is known to contribute to magnetic hyperfine fields [28] as well as to magnetic anisotropies [29].

In conclusion, we have studied magnetic ordering of monolayer-thick Fe islands on W(110) by nuclear resonant scattering of synchrotron radiation. At temperatures below 100 K these islands exhibit a perpendicular spin orientation. We attribute this to the interplay between the shape anisotropy and anisotropies induced by the peculiar elastic properties of this system. Moreover, the experiment has demonstrated that nuclear resonant scattering at modern synchrotron radiation sources is well suited to probe magnetism in the submonolayer regime. Further measurements with improved statistics will reveal more details about the hyperfine field distribution and, e.g., the critical behavior of the magnetic order in two-dimensional magnetic nanoparticles.

This work was partly supported by the European community (Brite/Euram III). We gratefully acknowledge the support of T. Asthalter and the staff of beam line ID18 during the experiment.

[1] F. J. Himpsel, J. E. Ortega, G. J. Mankey, and R. F. Willis, Adv. Phys. **47**, 511 (1998).
[2] *Metal Clusters at Surfaces,* edited by K. H. Meiwes-Broer (Springer, Berlin, 2000).
[3] *Ultrathin Magnetic Structures,* edited by J. A. C. Bland and B. Heinrich (Springer, Berlin, 1994), Vols. I and II.
[4] U. Gradmann, in *Handbook of Magnetic Materials,* edited by K. H. J. Buschow (Elsevier, Amsterdam, 1993), Vol. 7.
[5] M. Przybylski and U. Gradmann, Phys. Rev. Lett. **59**, 1152 (1987).
[6] M. Przybylski, I. Kaufmann, and U. Gradmann, Phys. Rev. B **40**, 8631 (1989); M. Przybylski, Hyperfine Interact. **113**, 135 (1998).
[7] W. Weber, D. Kerkmann, D. Pescia, D. A. Wesner, and G. Güntherodt, Phys. Rev. Lett. **65**, 2058 (1990).
[8] H. J. Elmers, J. Hauschild, and U. Gradmann, Phys. Rev. B **54**, 15 224 (1996).
[9] H. J. Elmers, G. Liu, and U. Gradmann, Phys. Rev. Lett. **63**, 566 (1989).
[10] M. Getzlaff, J. Bansmann, J. Braun, and G. Schönhense, Z. Phys. B **104**, 11 (1997).
[11] U. Gradmann, J. Korecki, and G. Waller, Appl. Phys. A **39**, 101 (1986).
[12] M. Przybylski and U. Gradmann, J. Phys. C **8**, 1705 (1988).
[13] H. J. Elmers, J. Hauschild, H. Höche, U. Gradmann, H. Bethge, D. Heuer, and U. Köhler, Phys. Rev. Lett. **73**, 898 (1994).
[14] W. Sturhahn and E. Gerdau, Phys. Rev. B **49**, 9285 (1994).
[15] L. Niesen, A. Mugarza, M. F. Rosu, R. Coehoorn, R. M. Jungblut, F. Roozeboom, A. Q. R. Baron, A. I. Chumakov, and R. Rüffer, Phys. Rev. B **58**, 8590 (1998).
[16] R. Rüffer and A. I. Chumakov, Hyperfine Interact. **97/98**, 589 (1996).
[17] A derivation of Eq. (1) will be given in a separate publication.
[18] U. van Bürck, D. P. Siddons, J. B. Hastings, U. Bergmann, and R. Hollatz, Phys. Rev. B **46**, 6207 (1992).
[19] S. W. Lovesey and S. P. Collins, *X-ray Scattering and Absorption by Magnetic Materials* (Clarendon Press, Oxford, 1996), p. 180.
[20] R. Röhlsberger, Hyperfine Interact. **123/124**, 455 (1999).
[21] C. P. Bean and J. D. Livingston, J. Appl. Phys. **30**, 120S (1959).
[22] J. G. Gay and R. Richter, Phys. Rev. Lett. **56**, 2728 (1986).
[23] Y. Park, S. Adenwalla, G. P. Felcher, and S. D. Bader, Phys. Rev. B **52**, 12 779 (1995); F. Bødker, S. Mørup, and S. Linderoth, Phys. Rev. Lett. **72**, 282 (1994).
[24] A. Q. R. Baron, A. I. Chumakov, H. F. Grünsteudel, H. Grünsteudel, L. Niesen, and R. Rüffer, Phys. Rev. Lett. **77**, 4808 (1996).
[25] A. Enders, D. Sander, and J. Kirschner, J. Appl. Phys. **85**, 5279 (1999).
[26] N. Weber, K. Wagner, H. J. Elmers, J. Hauschild, and U. Gradmann, Phys. Rev. B **55**, 14 121 (1997).
[27] D. Sander, R. Skomski, A. Enders, C. Schmidthals, D. Reuter, and J. Kirschner, J. Phys. D **31**, 663 (1998); D. Sander, A. Enders, and J. Kirschner, Europhys. Lett. **45**, 208 (1999); D. Sander, Rep. Prog. Phys. **62**, 809 (1999).
[28] S. C. Hong, A. J. Freeman, and C. L. Fu, Phys. Rev. B **38**, 12 156 (1988).
[29] H. J. Elmers and U. Gradmann, Surf. Sci. **304**, 201 (1994).